

Nonyl-and Dodecylamines Intercalated Bentonite and Illite From Turkey

Gülten AKÇAY, M. Kadir YURDAKOÇ*

*Department of Chemistry, Faculty of Arts & Sciences of Dicle University,
21280, Diyarbakır-TURKEY*

Received 14.05.1998

Bentonite and illite were interacted with nonyl- and dodecylammonium salt solutions to see how the alkylammonium ions became attached and oriented within the interlamellar space of the clays. X-ray diffraction analyses were carried out to obtain information on the interlamellar organization and orientation of the adsorbed alkylammonium compounds. Thermogravimetric analysis (TG, DTG) and Fourier Transform Infrared Analyses (FTIR) were performed to characterize the samples and to determine the amounts adsorbed by the clay samples. The modification process was effective in nonyl- and dodecylammonium bentonites. Alkylammonium ions were adsorbed in the interlamellar space of the clays. Regarding the orientation of the alkylammonium ions between the silicate sheets, it was found that the organic cation alkylchains were parallel to the silicate layer. Intercalation was generally greater with DA ions.

Introduction

Due to isomorphous substitution, clay minerals carry a permanent negative charge in their structural framework, which is balanced by exchange cations such as Na^+ , K^+ , Ca^{2+} and Mg^{2+} . The hydration of these inorganic exchange ions present in clays, and the nature of Si-O groups imparts a hydrophilic nature to the mineral surfaces. Because of this property, water is preferentially adsorbed by these surfaces, and non-polar organic compounds cannot compete with strongly held water for adsorption sites on the clay surfaces. As a result, natural clays are ineffective sorbents for poorly water-soluble organic contaminants. However, it is possible to modify the surface properties of clays greatly by neutralizing the anionic framework of layer silicates by using positively charged organic species such as primary aliphatic amine salts and alkylammonium ions¹⁻³. In the modified form, the clay surface may become organophilic and interact strongly with organic compounds.

The orientation of organic cations and some nonionic compounds at the clay surface has been extensively studied and it was found that the orientation of alkylammonium ions depends largely on their packing density. In relatively weakly charged clays such as montmorillonite and hectorite, the cations are oriented with the alkyl chains lying flat between the silica sheets. In moderately layer charged clays such as

* To whom all the correspondence should be addressed.

vermiculite, the chains are tilted regard to the surface, and when the surface has a high charge density, the increase in the number of adsorbed counterions causes their perpendicular orientation^{4,5}.

It appears that the first portion of the cationic amine is adsorbed onto clay by ion exchange; if more amine is added to the system, the clay can take up as much again, to a maximum of about twice the CEC (cation exchange capacity). The adsorption of surface active amines in excess of CEC was also found to be dependent on the chain length.

Besides being dependent on the alkyl chain length of the cation and the charge on the mineral layer, the arrangement of intercalated n-alkylammonium ions is also influenced by the method of preparation of the complex.

The intent of the present investigation was threefold. First bentonite and illite were interacted with nonyl- and dodecylammonium salt solutions to see how the alkylammonium ions became attached and oriented within the interlamellar space of the clays. Second, X-ray diffraction analyses were carried out to obtain information on the interlamellar organization and orientation of the adsorbed alkylammonium compounds. Third, thermo-gravimetric analysis and Fourier Transform Infrared Analyses (FTIR) were done to characterize the samples and to determine the adsorbed amounts by the clay samples, respectively.

Experimental Procedures

The bentonite was from the town of Reşadiye in Tokat-Turkey. Illite was supplied by the mineral Research and Exploration Institute of Turkey (MTA, 2650). The CECs of these samples were determined according to the ammonium acetate method⁶ to be 100 and 50 mEq/100g clay, respectively.

Preparation of Organo-Clays

The hydrochloride salt solutions of nonylamine and dodecylamine were prepared by mixing the appropriate amount of amine with 0.1N HCl solutions. The hydrogen ion concentration was approximately 20% in excess of the stoichiometric amount to ensure complete conversion of the amine to the salt form. Previously dried (110 °C, 24 h) and desiccated clays were mixed with nonyl- and dodecylammonium chloride concentrations of 5 mEq greater than the CEC of the clays. The mixtures were subjected to mechanical shaking for 48 h at a constant temperature of 25 °C.

The clay suspensions were separated from the mixture by centrifugation, washed with ethanol/water, dried at 40 °C for 24 h and mechanically ground to 140 mesh.

These organo-clays were denoted as nonylammonium bentonite (NAB), dodecylammonium bentonite (DAB) for bentonite; nonylammonium illite (NAI); dodecylammonium illite (DAI) for illite, respectively.

The BET surface areas were determined by nitrogen adsorption at 77K in a Ströhlein Areameter.

Thermogravimetric analyses (TG, DTG) were carried out on samples weighing <20 mg under a flow of N₂ (10 mL min⁻¹) at a heating rate of 15 °C min⁻¹ using a SHIMADZU TGA-50 Thermogravimetric Analyser.

The XRD powder profiles were obtained with a Siemens D-500 diffractometer using nickel filtered Cu K_α radiation in EBI, Karlsruhe University, Germany.

The FTIR spectra of samples were recorded in KBr (1mg sample/250mg KBr) pellets using MAIDAC 1700M FTIR spectrometer in the range 4000-400 cm⁻¹ with a resolution of 2cm⁻¹ after 50 scans.

Results and Discussion

BET specific surface area values of the samples are given in Table 1. It can be clearly seen that there was a decrease in the order of nonyl- and dodecylammonium ion treated samples. This may be due to the blocking of the micro pore openings on the surface by large organic counterions, or formation of macro porous structure.

Thermogravimetric Studies

Figures 1a and 1b present the thermograms and derivative thermograms for the decomposition of nonyl- (NA) and dodecylammonium chlorides (DA) which exhibit decomposition maxima near 308 and 300 °C, respectively.

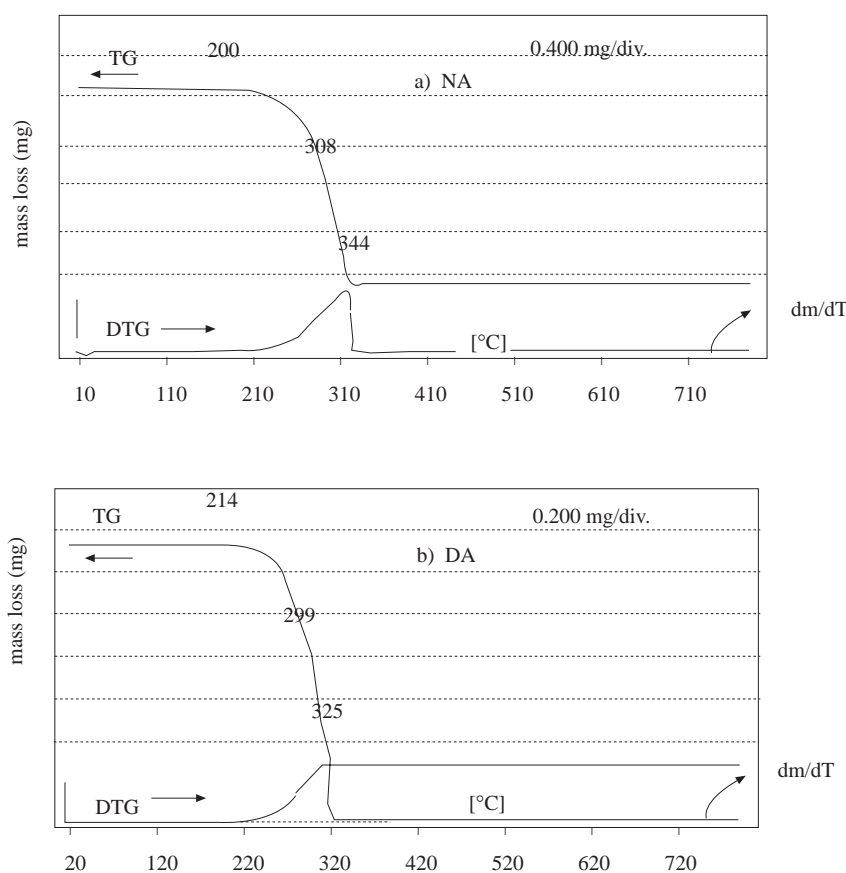


Figure 1. TG and DTG Thermograms of (a) Nonyl- (NA) and (b) Dodecylammonium (DA) Chlorides

The TG and DTG thermograms of B, NAB and DAB are shown in Figures 2a, 2b and 2c. Figure 2a exhibits desorption maxima near 44, 80 and 685 °C which can be attributed to the desorption of physically adsorbed water and the dehydroxylation of the aluminosilicate layer, respectively. The peak at 80 °C is not fully understood, but may be the result of the desorption of water a divalent or trivalent ion. Such types of peak were also found at 100 °C⁷. These two peaks were lower after the NA and DA treatment. The DTG thermogram for NAB and DAB (Figures 2b-2c) exhibited two peaks, prior to the dehydroxylation peak split into two peaks, at 335 and 343 °C for the decomposition of the NA and DA ions respectively. On the other

hand, in samples of NAB and DAB, the dehydroxylation peak split into two peaks at 622 and 722 °C for NAB and 618 and 718 °C for DAB. The peaks were attributed to water and carbon dioxide produced as the carbonaceous deposit remaining on the surface after the partial desorption and decomposition of the alkylammonium ions around 330-340°C. Dehydroxylation may be affected by the exchange cation after the NA and DA treatment. The TG and DTG of illite, NAI and DAI are given in Figure 3. Figure 3a presents the TG and DTG for the desorption of water from illite, which in general exhibit desorption maxima near 45 and 625 °C which can be attributed to the desorption of physically adsorbed water, and the dehydroxylation of the aluminosilicate layer, respectively. An additional desorption maximum near 150 °C was also observed. The origin of this peak is unclear, but probably was due to the desorption of water from a divalent or trivalent ion, but was removed after the exchange with NA and DA ions. The total loss of mass in I was <1% and 4% respectively while the total loss of mass in NAI and DAI was 5.23% and 6.40%. In samples NAI and DAI, the dehydroxylation maximum shifted to lower temperatures such as 588 and 578 °C respectively. This could reflect the onset of dehydroxylation at a lower temperature due to the the nonyl- and dodecylammonium ions. It can be seen from Figures 3b and 3c that the decomposition of NA and DA ions covered progressively a broad temperature range of 180-450 °C.

Figure 4 shows the XRD pattern of B, NAB and DAB samples. The XRD pattern of bentonite shows that it contains some amounts of illite which has a basal reflection of $d(001)=10.03 \text{ \AA}$ at a 2θ value of 8.806 with a $I=56 \%$. In Figures 4b and 4c, the basal reflection lines of montmorillonite $d(001)$, were observed at $2\theta=6.585$, $d=13.41 \text{ \AA}$ and $I=100.0\%$ for NAB, and also at $2\theta=6.353$, $d=13.90 \text{ \AA}$ and $I=70.0\%$ for DAB samples.

Relationships between layer charge and the interlayer expansion of clay minerals by n-alkylamine hydrochlorides were determined and it was found that depending on the alkyl chain length and the mineral charge, the alkyl chains of these cations may form either monolayers, bilayers, pseudotrimolecular layers, or paraffin complexes^{4,8}. For NAB and DAB, the organic cation alkylchains were parallel to the silicate layer. These organo-clays had basal spacings $d(001)$ of 13.4 and 13.9 Å by the XRD analysis, respectively. This implies an external organic thickness of 3.9 Å for NAB and 4.1Å for DAB, besides an inorganic one of 9.5 Å.

The basal separation of the complexes with alkylammonium ions gave no evidence that more than a single layer of cations was present in the interlamellar space, if it was assumed that the thickness of an individual montmorillonite lamella was 9.5 Å and the van der Waals' thickness of the methyl or methylene group was 4 \AA^{9-11} . The adsorbed cations could therefore be accommodated within a single layer at maximum adsorption.

Figure 5 shows the XRD patterns of I, NAI and DAI samples. Identification of the mineral content of the illite sample was done by referring to JCPDS Cards No 2-0462, 9-334 and 2-42. The basal reflection line of illite $d(001)$ was observed at $2\theta=8.889$, $d=9.94 \text{ \AA}$ and $I=25.5\%$, and other lines were in agreement with the above reference cards. This implies that the sample was composed of the illite mineral and very large amounts of quartz.

On the other hand, the basal reflection lines of NAI and DAI were observed at $2\theta=8.742$, $d=10.11\text{ \AA}$, $I=42.2\%$, $2\theta=8.563$, $d=10.32 \text{ \AA}$, $I=46.1\%$, respectively. The increase was in the order of $\text{DAI} < \text{NAI} < \text{I}$. However, some lines were also observed at $2\theta=6.098$, $d=14.48 \text{ \AA}$ for NAI, and $2\theta=6.932$, $d=12.74 \text{ \AA}$; $2\theta=4.743$, $d=18.61 \text{ \AA}$ for DAI, but their integration ratios were less than 1 percent.

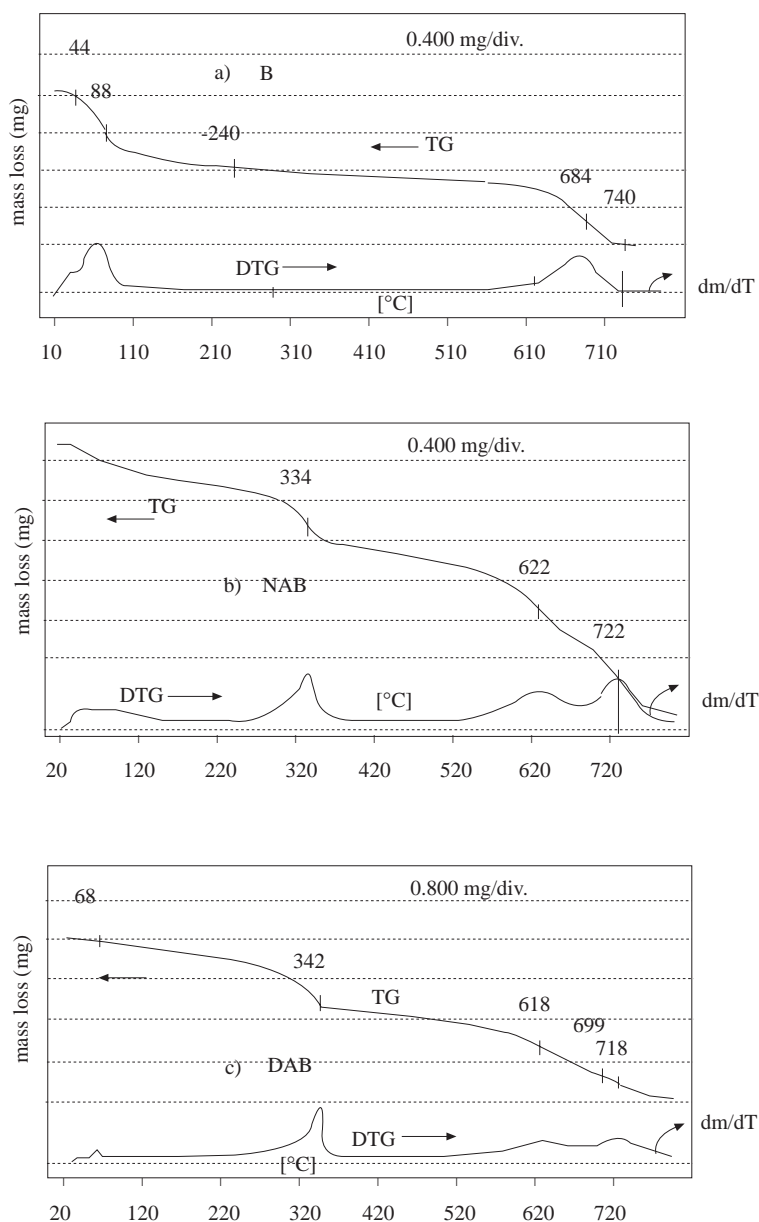


Figure 2. TG and DTG Thermograms of the Samples (a) Bentonite (B), b) NAB, c) DAB

FTIR spectra of the bentonite samples are given in Figure 6. In the FTIR spectrum of B, the Al-Al-OH stretching frequency was observed at 3620 cm^{-1} , while the bending frequency was at 915 cm^{-1} . This can be considered characteristic of a dioctahedral smectite¹². The bands at 3460 and 1640 cm^{-1} were the OH stretching and bending frequencies of the hydration water. The intense broad between 1100 and 1020 cm^{-1} were those of the Si-O stretching frequencies. The tetrahedral bending modes were at 530 cm^{-1} for Si-O-Al, at 470 cm^{-1} for Si-O-Mg, and at 428 cm^{-1} for Si-O-Si¹³. We note that the intensity of the band at 470 cm^{-1} was higher than that observed normally for a dioctahedral smectite. This may be due to the presence of some illite in the sample. It has been suggested that the OH bending frequencies in dioctahedral 2:1 layer silicates were assigned in the following: Al^{III}-Al^{III}-OH near 915 cm^{-1} ; Fe^{III}-Al^{III}-OH near 880 cm^{-1} ; Mg^{II}-Al^{III}-OH near 835 cm^{-1} , and Mg^{II}-Fe^{III}-OH near 795 cm^{-1} . In the IR spectra of NAB and

DAB, all the bands belonging to the original bentonite were reserved. The band expected at 3030 cm^{-1} for the NH_4^+ stretching was not observed in these samples. The band from structural OH at 3620 cm^{-1} of NAB and DAB samples shifted to 3640 cm^{-1} . The bands at 2930 and 2855 cm^{-1} were assigned as the C-H stretching of methyl and methylene groups in NA and DA salts. The band at 3280 cm^{-1} may be assigned to the stretching mode of the NH_4^+ . On the other hand, the band at 1470 cm^{-1} was due to the bending vibration of NH_4^+ , or deformation bands of the methyl and methylene groups. They can also coincide with each other. Since the frequency of the CH_3 and CH_2 bands remains sensibly constant whether or not water is present, hydrogen bonding between these groups and water and between these and surface oxygens is not important.

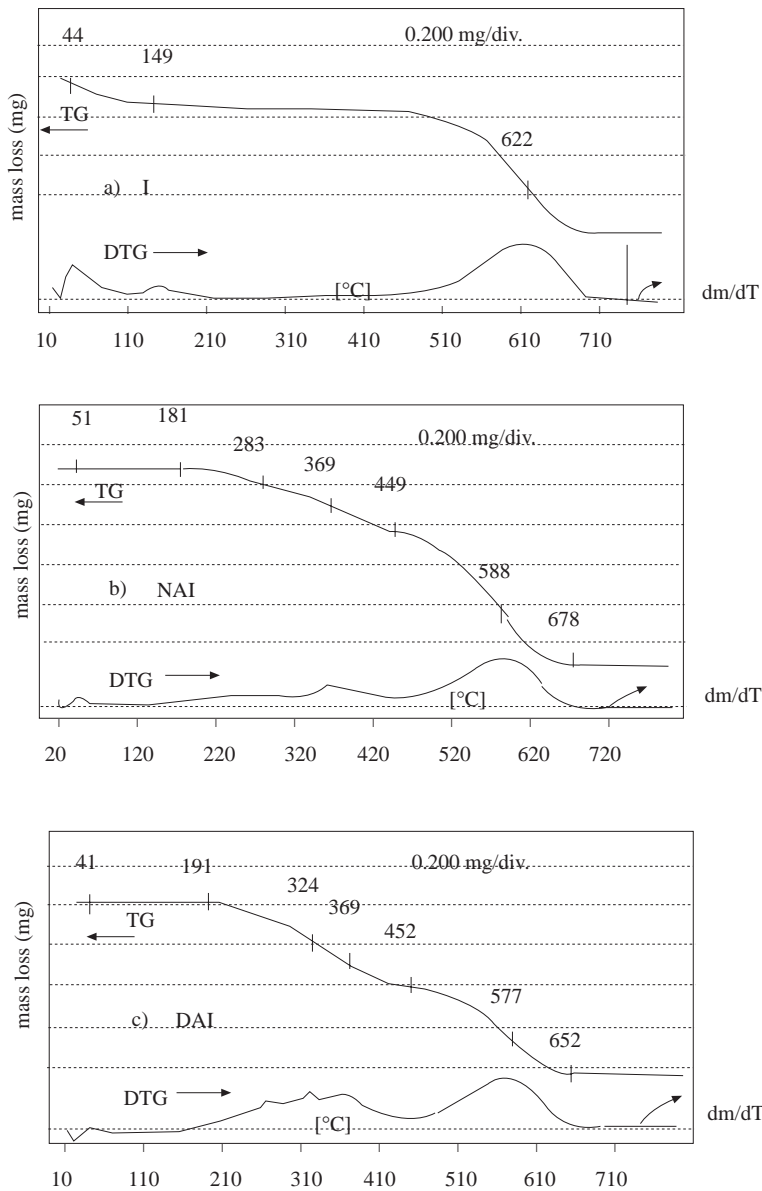


Figure 3. TG and DTG Thermograms of the Samples (a) Illite (I), (b) NAI, (c) DAI

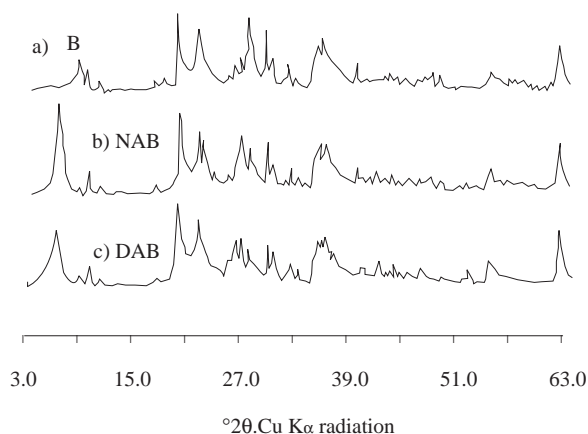


Figure 4. X-Ray Powder Diffraction Patterns of B, NAB and DAB

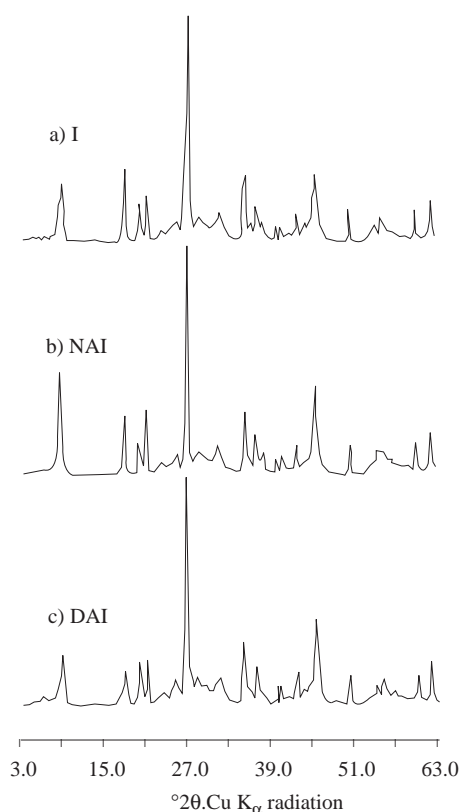


Figure 5. X-Ray Powder Diffraction Patterns of I, NAI and DAI

FTIR spectra of the illite samples are given in Figure 7. The composition of illite was quite variable, as was its IR spectrum. Nevertheless, two main types of spectrum were identified, being associated with muscovite-like and phengite-like illites. The illite spectra can range between these two types and may show even weaker adsorption bands near 825 and 750 cm^{-1} . Consequently, it can be difficult to identify the type of illite. These two bands were clearer in the case of NAI and DAI samples. These bands originate in Al-Mg-OH deformation and Al-O-Si in plane vibration¹⁴. Diagenetic illites sometimes contain interlayer NH_4^+ ions replacing K^+ , the NH_4^+ ions absorbing at 3260 and 1430 cm^{-1} ¹⁵.

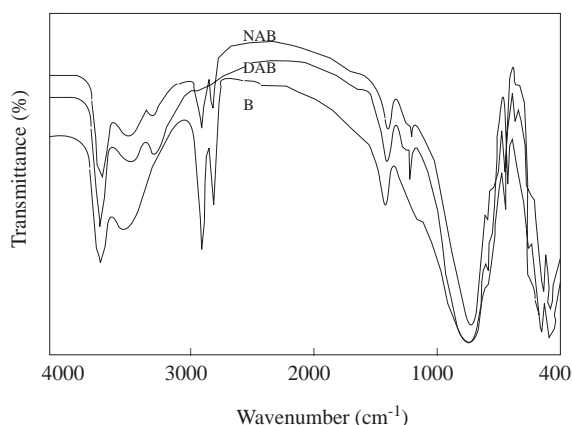


Figure 6. FTIR Spectra of B, NAB and DAB

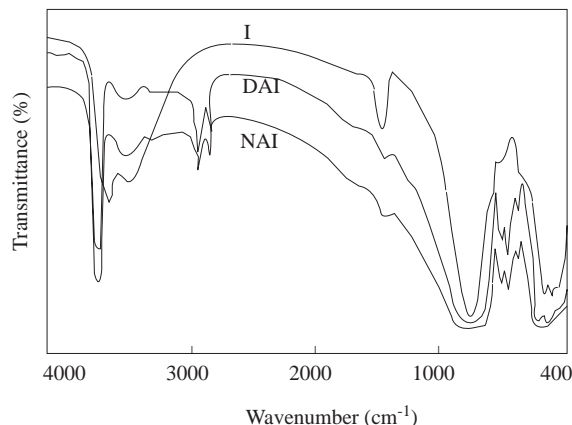


Figure 7. FTIR Spectra of I, NAI and DAI

Table 1. Chemical Composition of the Clays, wt%

Sample	SiO ₂	Al ₂ O ₃	Fe ₂ O ₃	TiO ₂	MgO	CaO	Na ₂ O	K ₂ O	Ignition	Total
Bentonite	58.78	19.24	3.58	0.37	2.13	4.21	2.73	1.35	7.48	99.87
Illite	65.05	19.11	2.12	0.20	1.34	0.72	0.34	5.54	5.50	99.92

Table 2. BET Surface area values of the samples

Sample	S(m ² g ⁻¹)	Sample	S(m ² g ⁻¹)
B	28.2	I	10.1
NAB	15.6	NAI	4.6
DAB	8.4	DAI	3.9

The broad OH-stretching band near 3625 cm⁻¹, ranging below 3600 cm⁻¹ in some instances coupled with the 825, 750 cm⁻¹ doublet is almost certainly diagnostic. The bands at 3600 and 3414 cm⁻¹ in the illite spectrum belonging to the hydroxyl groups bonded to the illite crystal and adsorbed water respectively. The deformation band of adsorbed water at 1640 cm⁻¹ was disturbed in the spectra of NAI and DAI and shifted to 1620 cm⁻¹. The bands in the 850-600 cm⁻¹ region of NAI and DAI were resolved more clearly than I. The OH-stretching bands in NAI and DAI appeared at 3630 cm⁻¹ and were very sharp compared with the original IR spectrum of illite. The other bands at 2930 (with a shoulder at 2958 cm⁻¹) and 2856 cm⁻¹ were assigned as C-H stretching vibrations of CH₃ and CH₂ groups. The weak bands at 3230 at 1466 cm⁻¹ may be due to the NH₄⁺ ion.

Conclusion

From the experimental data described above, it is possible to modify the clays in some respect with n-alkylammonium salts. The modification process occurred in such a way that the alkylammonium ions were adsorbed on the interlamellar space of the clays. The adsorption was through an exchange reaction between the inorganic cations on the clay and the alkylammonium ions in the solution. According to the X-ray data for NAB and DAB, the organic cation alkylchains were parallel to the silicate layer. The schematic representation of layered structure of organo-clays can be seen in Figure 8. There was a small change in the basal reflection lines of NAI and DAI. However, intercalation was generally greater with DA ions.

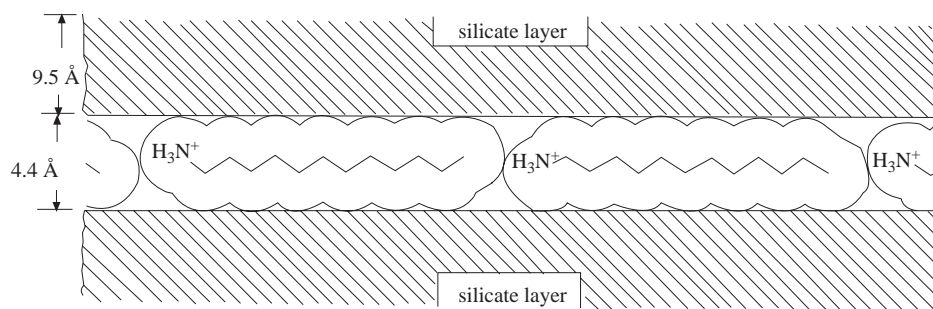


Figure 8. The Schematic Representation of Layered Structure of DAB

Acknowledgements

The authors are indebted to Prof. Dr. Ing. Dieter Hönicke for providing the XRD analysis data, and Dr. Holger Mietzel for the BET analysis.

References

1. C. T. Cowan and D. White, **Trans. Faraday Soc.** **54**, 691-697 (1958).
2. B. K. G. Theng, D. J. Greenland and J. P. Quirk, **Clay Miner.** **7**, 1-17 (1967).
3. R. M. Barrer and J. S. S. Reay, **Trans. Faraday Soc.** **53**, 1253-1261 (1957).
4. G. Lagaly, **Solid State Ionics** **22**, 43-51 (1986).
5. G. Lagaly, **Clays Clay Miner.** **30**, 215-222 (1982).
6. R. C. Mackenzie, **J. Colloid Sci.** **6**, 219-222 (1951).
7. C. Breen, **Clay Miner.** **26**, 473-486 (1991).
8. G. Lagaly, **Clay Miner.** **11**, 173-187 (1981).
9. R. Greene-Kelly, **Trans. Faraday Soc.** **51**, 412-424 (1955).
10. G. W. Brindley and R. W. Hoffmann, **Clays Clay Miner.** **9**, 546-556 (1962).
11. L. Pauling, **"The Nature of the Chemical Bond"**, 3rd.Ed., Cornell University Press, Ithaca, N. Y., 1960.
12. G. A. Borchardt, **"Montmorillonite and other smectite minerals"** in *Minerals in Soil Environments*: Ed. Dixon, J. B. And Weed, S. B., Soil Science Society of America, Madison, Wisconsin, pp. 229-330, 1977.
13. H. W. Van der Marel and H. Beutelspacher, **"Atlas of Infrared Spectroscopy of Clay Minerals and Their Admixtures"** Elsevier, Amsterdam, pp. 31-58, 1976.
14. V. C. Farmer, **"The layers silicates"** in *The Infrared Spectra of Minerals*, Mineralogical Society, London pp. 331-363, 1974.
15. P. H. Nadeau and D. C. Bain, **Clays and Clay Miner.** **34**, 455-465 (1986).

CONTENTS

<i>Impedance Characteristics of Conducting Polypyrrole-poly(ethylvinylether) Graft Films</i>	1
E. KALAYCIOĞLU, L. TOPPARE, T. GRCHEV, M. CVETKOVSKA, Y. YAĞCI	
<i>¹³C- and ³¹P-NMR Study of Tetracarbonylbis(diphenylphosphino)alkanemetal(0) Complexes of The Group 6 Elements</i>	9
Z. ÖZER, S. ÖZKAR	
<i>Chemical Constituents of Centaurea cuneifolia</i>	15
Ü. ASLAN, S. ÖKSÜZ	
<i>Effects of Ozonation on COD Elimination of Substituted Aromatic Compounds in Aqueous Solution</i>	21
Ş. GÜL, O. SERİNDAG, H. BOZTEPE	
<i>An Efficient Acetylation of Primary and Secondary Aliphatic Alcohols with Acetic Anhydride in the Presence of Graphite Bisulphate</i>	27
H. SEÇEN, A. H. KALPAR	
<i>Thermodynamics of the Dissociation of Chromium Soap Solutions in Benzene-Dimethyl Formamide</i>	31
H. TOPALLAR, Y. BAYRAK	
<i>The Effect of phosphate Ions (PO₄³⁻) on the Corrosion of Iron in Sulphate Solutions</i>	41
G. KILINÇEKER, B. YAZICI, M. ERBİL, H. GALİP	
<i>The Recovery of Copper and Cobalt from Oxidized Copper Ore and Converter Slag</i>	51
B. ZİYADANOĞULLARI, R. ZİYADANOĞULLARI	
<i>The Role of Electrolytically Co-Deposited Platinum-Palladium Electrodes On The Electrooxidation Of D. Glucose In Alkaline medium: A Synergistic Effect</i>	57
İ. BECERİK	
<i>Synthesis and Spectral Characterisation of Novel Azo-Azomethine Dyes</i>	67
H. KARAER, İ. E. GÜMRÜKÇÜOĞLU	
<i>Electrooxidation of Linear Alkyl Benzene Sulfonate (LAS) on Pt Electrodes</i>	73
B. YAZICI, S. ZOR	
<i>The Application of a Scanning Electron Microscope With an Energy Dispersive X-Ray Analyser (SEM/EDXA) For Gunshot Residue Determination on Hands For Some Cartridges Commonly Used In Turkey</i>	83
K. GÖKDEMİR, E. SEVEN, Y. SARIKAYA	
<i>Electrochemical Preparation and Sensor Properties of Conducting Polyaniline Films</i>	89
M. ÖZDEN, E. EKİNCİ, A. E. KARAGÖZLER	
<i>Nepetalactones and Other Constituents of Nepeta nuda ssp. albiflora</i>	99
G. KÖKDİL, S. M. YALÇIN, G. TOPÇU	
<i>Nonyl-and Dodecylamines Intercalated Bentonite and Illite From Turkey</i>	105
G. AKÇAY, M. K. YURDAKOÇ	